

See discussions, stats, and author profiles for this publication at: <https://www.researchgate.net/publication/232810074>

The Factor H Binding Protein of *Neisseria meningitidis* Interacts with Xenosiderophores in Vitro

ARTICLE in BIOCHEMISTRY · NOVEMBER 2012

Impact Factor: 3.02 · DOI: 10.1021/bi301161w · Source: PubMed

CITATIONS

8

READS

108

11 AUTHORS, INCLUDING:



Daniele Veggia

GlaxoSmithKline plc.

35 PUBLICATIONS 1,084 CITATIONS

[SEE PROFILE](#)



Francesca Cantini

University of Florence

42 PUBLICATIONS 1,395 CITATIONS

[SEE PROFILE](#)



Vincenzo Nardi-Dei

Novartis Vaccines

26 PUBLICATIONS 837 CITATIONS

[SEE PROFILE](#)



Kate Seib

Griffith University

1 PUBLICATION 8 CITATIONS

[SEE PROFILE](#)

The Factor H Binding Protein of *Neisseria meningitidis* Interacts with Xenosiderophores in Vitro

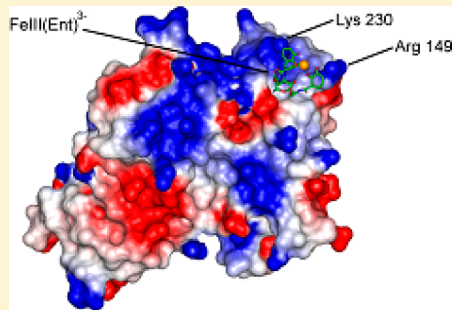
Daniele Veggi,[†] Maria A. Gentile,[†] Francesca Cantini,[‡] Paola Lo Surdo,[†] Vincenzo Nardi-Dei,[†] Kate L. Seib,[†] Mariagrazia Pizza,[†] Rino Rappuoli,^{*,†} Lucia Banci,^{*,‡} Silvana Savino,[†] and Maria Scarselli[†]

[†]Novartis Vaccines and Diagnostics, Via Fiorentina 1, Siena, Italy

[‡]Magnetic Resonance Center, University of Florence, Via L. Sacconi 6, Sesto Fiorentino, Italy

Supporting Information

ABSTRACT: The factor H binding protein (fHbp) is a key virulence factor of *Neisseria meningitidis* that confers to the bacterium the ability to resist killing by human serum. The determination of its three-dimensional structure revealed that the carboxyl terminus of the protein folds into an eight-stranded β barrel. The structural similarity of this part of the protein to lipocalins provided the rationale for exploring the ability of fHbp to bind siderophores. We found that fHbp was able to bind in vitro siderophores belonging to the cathecolate family and mapped the interaction site by nuclear magnetic resonance. Our results indicated that the enterobactin binding site was distinct from the site involved in binding to human factor H and stimulates new hypotheses about possible multiple activities of fHbp.



Neisseria meningitidis is an obligate human pathogen that can cause severe and sometimes fatal septicaemia and meningitis.^{1–3} Meningococcal serogroup B has long been identified as an important cause of disease in many parts of the world. However, vaccine development has been hindered by the biochemistry of its capsular polysaccharide^{4–6} and the difficulties inherent in identifying appropriate surface protein antigens.⁷ The use of reverse vaccinology to select antigens suitable for vaccine development led to identification of a number of novel proteins.⁸ As a result a multicomponent vaccine has been proposed,⁹ which includes among the other antigens fHbp, a surface-anchored lipoprotein previously termed genome-derived neisserial antigen 1870 (GNA1870),⁸ or LP20286.¹⁰ fHbp is able to induce a strong immune response in animals and humans.^{11–13}

fHbp is prone to sequence variability, so that three distinct variants of the protein can be recognized in the meningococcal population.¹⁴ Each variant is, however, able to bind human factor H (fH), a negative regulator of the alternative complement pathway.¹⁵ fH is a 150 kDa polypeptide composed of 20 domains of ~60 amino acid each¹⁶ called short consensus repeats (SCRs) arranged in a consecutive fashion. fH is normally present at high concentrations in human serum.¹⁷ Its binding to the surface of human cells protects them from autoimmune attack.^{17,18} Meningococci evolved the ability to capture human fH on their surface thanks to the direct interaction with fHbp. It has been shown that fH binds fHbp via SCR6 and -7.¹⁹ Such interaction allows the meningococcus to evade the innate immunity of the host.²⁰

The three-dimensional structure of fHbp, free^{21–23} or in complex with SCR6 and -7 of human factor H,¹⁹ showed that the meningococcal protein consists of two domains connected by a flexible linker. While the N-terminal domain adopts an

elongated “barrel-like” structure characterized by the presence of long loops and by extensive flexibility, the C-terminal portion of the molecule is arranged in a well-defined β barrel that is stabilized by a regular network of hydrogen bonds. The structure of the C-terminal domain shows a remarkable similarity to those of lipocalins.²⁴ Lipocalins form a wide family of proteins expressed by plants, fungi, bacteria, vertebrates, and invertebrates^{25,26} that participate in many biological functions, including binding to siderophores. With the name siderophores are collectively indicated a variety of organic chelators that have a strong affinity for ferric iron. This metal is essential for the growth and development of almost all living organisms, including bacteria that during infection cannot freely access the host iron reservoir, as the metal is tightly sequestered by proteins or hemes in the host. Because of this competition between pathogenic bacteria and the human host for ferric iron uptake, siderophores are considered to be virulence factors because of their capacity to feed microorganisms with this metal.²⁷

The structural similarity of fHbp to lipocalins prompted us to investigate the possible role of fHbp as a siderophore-binding protein. In this work, we initially explored the affinity of recombinant meningococcal fHbp for different siderophores in vitro. Our results show that the protein is able to bind enterobactin, a feature that is shared with its orthologue in *Neisseria gonorrhoeae*. These observations suggest that fHbp could be involved in iron uptake and for this reason play an important role in bacterial survival in the human body.

Received: August 28, 2012

Revised: October 31, 2012

Published: November 2, 2012

MATERIALS AND METHODS

fHbp Expression and Purification. The *fHbp* alleles were amplified by polymerase chain reaction from the chromosomal DNA of *N. meningitidis* strains MCS8, 2996, and M1239, while the chromosomal DNA of *N. gonorrhoeae* strain FA1090 was used to amplify the gonococcal gene. All the alleles were cloned into the pET21b vector (Novagen) under the control of the T7 promoter. Recombinant fHbp was expressed in the *Escherichia coli* BL21(DE3) strain as a C-terminal histidine fusion. Protein expression was induced by isopropyl 1-thio- β -D-galactopyranoside (IPTG) (Sigma), and then fHbp was purified by nickel chelating affinity chromatography using a HisTrap HP column (GE Healthcare) followed by cationic exchange chromatography. The purified protein was dialyzed in PBS buffer. For NMR analysis, the BL21(DE3) *E. coli* clone was grown in ISOGRO ^{15}N (Sigma). After protein purification, the final product was dialyzed in 20 mM sodium phosphate (pH 7.2), a specific requirement for NMR. Unlabeled variant 1 fHbp was purified following the same procedure, while fHbp variants 2 and 3 and the gonococcal isoform were purified by nickel chelating affinity chromatography and then anionic exchange chromatography and finally dialyzed in phosphate-buffered saline (PBS).

Native Gel Electrophoresis. Samples containing 100 μg of purified full-length fHbp-his were mixed and incubated for 1 or 8 h at room temperature, at a 1:1 molar ratio with commercially available ferric enterobactin [$\text{Fe}^{\text{III}}(\text{Ent})^{3-}$], ferric salmochelin, ferric yersiniabactin [$\text{Fe}^{\text{III}}(\text{Yers})$], and ferric aerobactin [$\text{Fe}^{\text{III}}(\text{Aer})$], all acquired from EMC microcollections GmbH, in PBS. Then the samples were mixed with Tris-glycine native sample buffer and loaded on Novex Tris-glycine or Novex Tris-acetate native gels (Invitrogen). Gels were run at 150 V constantly for 2 h and stained with SimplyBlue Safe Stain (Invitrogen).

Surface Plasmon Resonance (SPR) Analysis. All SPR experiments were performed using a Biacore T100 instrument (GE Healthcare) equilibrated at 25 °C. fHbp proteins were immobilized on the sensor surface as ligands, and siderophores were injected as analytes in optimized running buffer that consisted of PBS (pH 7.4), 0.05% P-20 detergent, and 2% methanol. For each titration, fHbp proteins were first covalently immobilized by amine coupling on a carboxymethylated dextran sensor chip (CM-5, GE Healthcare). Amine coupling reactions for immobilization of fHbp were performed using purified proteins at ~10 $\mu\text{g}/\text{mL}$ in 10 mM sodium acetate buffer (pH 5.5) injected at a rate of 5 $\mu\text{L}/\text{min}$ until ~2000 response units (RU) were captured. The blank (reference) surface was constructed similarly, although without fHbp.

A buffer optimization was necessary to run titration experiments because a growing nonlinear analyte response was observed upon binding, and the resulting sensorgrams could not be fit with any standard evaluation method. Preparing the initial analyte stock in a 100% methanol solution and then diluting the stock to a final methanol concentration of 2% in running buffer resolved this issue (PBS and 0.05% P-20).

Titration experiments were performed by injecting $\text{Fe}^{\text{III}}(\text{Ent})^{3-}$ prepared at increasing concentrations in optimized running buffer at a flow rate of 50 $\mu\text{L}/\text{min}$. Following each injection, sensor chip surfaces were regenerated with a 30 s injection of 10 mM NaOH. Each titration series contained 10–12 analyte injections, with maximal used siderophore concentrations of 280 μM . Data were analyzed using Biacore

T100 Evaluation (GE Healthcare); a blank injection of buffer only was subtracted from each curve, and reference sensorgrams were subtracted from experimental sensorgrams to yield curves representing specific binding. Steady-state analysis was used to plot the equilibrium binding response (R_{eq}) against analyte concentration to obtain the dissociation constants (K_D) (see the Supporting Information for details).

Ferric yersiniabactin, ferric aerobactin, and iron free enterobactin were tested as a single injection at 100 μM over immobilized proteins, and binding with $\text{Fe}^{\text{III}}(\text{Ent})^{3-}$ at the same concentration was used for comparison. Similarly, fH (domains 6 and 7) was injected at a concentration of 100 nM over immobilized gonococcal fHbp and compared for binding with a 100 μM $\text{Fe}^{\text{III}}(\text{Ent})^{3-}$ injection.

NMR Interaction Studies. The interaction of $\text{Fe}^{\text{III}}(\text{Ent})^{3-}$, iron free enterobactin (apo-Ent), and ferric $\text{Fe}^{\text{III}}(\text{Yers})^{3-}$ with ^{15}N -labeled fHbp was investigated by NMR spectroscopy performed at 298 K on Bruker Avance 900 and 800 MHz spectrometers, at proton nominal frequencies of 899.20 and 800.13 MHz, respectively, using triple-resonance (TXI 5 mm) cryoprobes equipped with pulsed-field gradients along the z -axis.

All titrations were performed with 0.5 mM ^{15}N -labeled fHbp protein samples by adding siderophores up to an fHbp:siderophore molar ratio of 1:5. ^1H and ^{15}N resonance assignments for the fHbp protein were available.²³ All samples were in 20 mM phosphate buffer (90% H_2O and 10% D_2O) at pH 7.2. All two-dimensional spectra were processed using TOPSPIN (Bruker BioSpin).

The information obtained from the NMR interaction studies between fHbp and $\text{Fe}^{\text{III}}(\text{Ent})^{3-}$ was used as input for generating a model of the adduct through molecular docking. Docking calculations between fHbp and $\text{Fe}^{\text{III}}(\text{Ent})^{3-}$ were performed with HADDOCK2.0.²⁸ Twenty conformers of the fHbp solution structure (PDB entry 2KC0) and the PDB coordinates of the siderophores extracted from the crystal structure on the human siderocalin NGAL complexed with $\text{Fe}^{\text{III}}(\text{Ent})^{3-}$ (PDB entry 3CMP) were used as input. The topologies and parameter files for $\text{Fe}^{\text{III}}(\text{Ent})^{3-}$, necessary to run HADDOCK2.0, were generated by PRODRG (<http://davapc1.bioch.dundee.ac.uk/prodrg/>)²⁹ using the PDB coordinates extracted from the 3CMP crystal structure. The docking calculations in HADDOCK were driven by nine active and nine passive residues (Table S1 of the Supporting Information), which were used to generate ambiguous interaction restraints, as defined in the HADDOCK protocol.^{9,30} The active residues are those experimentally identified to be involved in the interaction between fHbp and $\text{Fe}^{\text{III}}(\text{Ent})^{3-}$ and solvent-accessible, i.e., solvent-exposed residues whose line widths of the NH signals increase upon addition of paramagnetic $\text{Fe}^{\text{III}}(\text{Ent})^{3-}$. The passive residues are all solvent-accessible surface neighbors of active residues. The solvent accessibility of fHbp was calculated with NACCESS.³¹ Flexible regions of the proteins were defined on the basis of active and passive residues and two preceding and following residues. Additional distance restraints with an upper bound distance of 2.0 Å were defined between the Fe^{III} atom and the six catechol oxygens according to previously reported protocols.^{32–35}

During the initial rigid-body docking calculation, the intermolecular interactions have been scaled down to a value of 0.01. In this phase, 1000 structures of the complex were generated and the best 200 in terms of total intermolecular energy were further submitted to semiflexible simulated

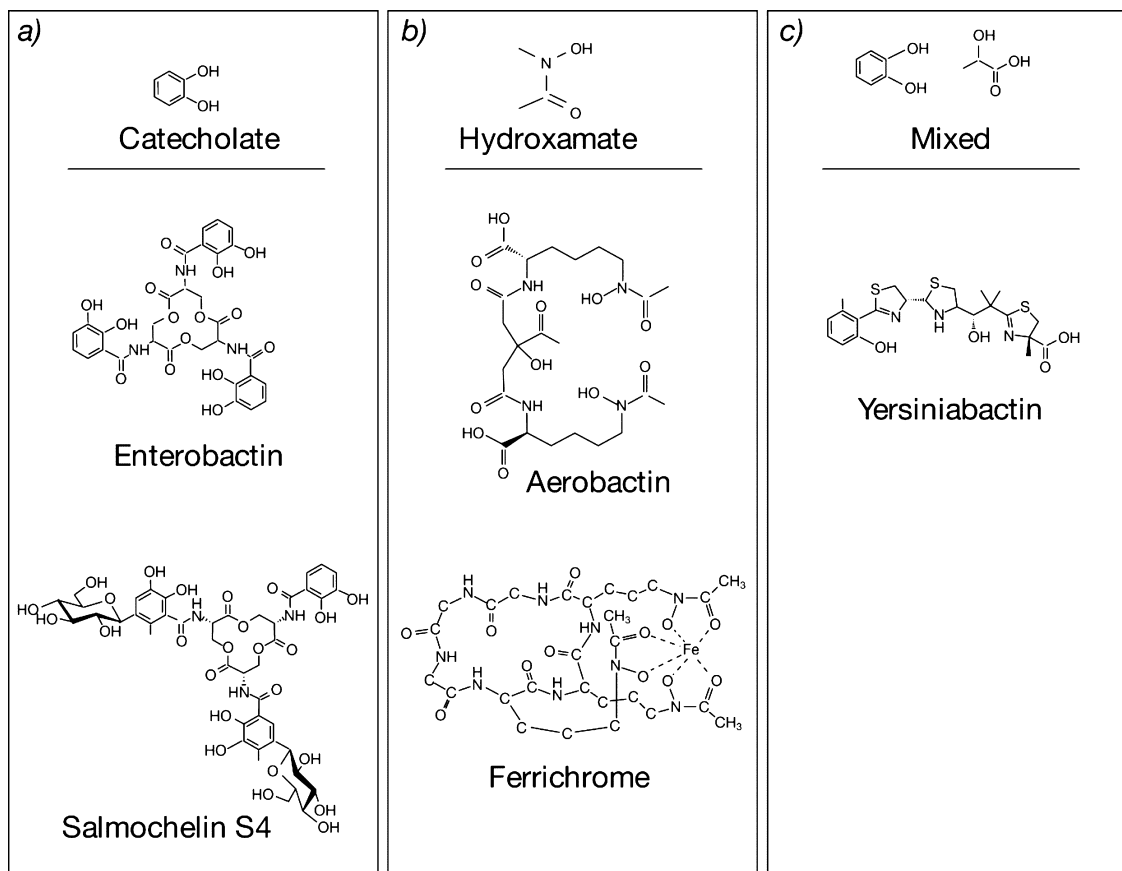


Figure 1. Prototypical members of the main siderophore classes. (a) Chelating groups are represented by three catecholate units. (b) Ligating groups include the oxygen atoms of hydroxamate. (c) Siderophores with mixed ligands and heterocyclic chelating groups.

annealing and final refinement in water. The initial temperature for the second torsion angle dynamic (TAD) cooling step with a flexible side chain at the interface was set up to 500 K. The molecular dynamics trajectory steps for rigid body high-temperature TAD and during the first rigid body cooling stage were set up to zero, while the numbers of MD steps during the second and third cooling stages with flexible side chains at the interface were set up to 500. The final 200 structures were then clustered using a cutoff of 2.0 Å of the root-mean-square deviation (rmsd) among any structure of a cluster. The docking solution could be divided into two clusters, which were ranked on the basis of the average HADDOCK score. Table S2 of the Supporting Information reports the statistics calculated over the best four models of each cluster.

RESULTS

fHbp–Enterobactin Interaction Revealed by Native Polyacrylamide Gel Electrophoresis (PAGE). On the basis of their chemical structure (Figure 1), siderophores can be subdivided into catecholates, hydroxamates, or mixed classes. Cathecolates (enterobactin and salmochelin), a hydroxamate (aerobactin), and a mixed siderophore (yersiniabactin) were selected as representative members of the respective classes and tested for their ability to bind to recombinant meningococcal fHbp by native gel electrophoresis.

A faster gel migration was detected for fHbp after incubation in the presence of enterobactin and, to a lesser extent, after incubation with salmochelin (Figure 2). On the other hand,

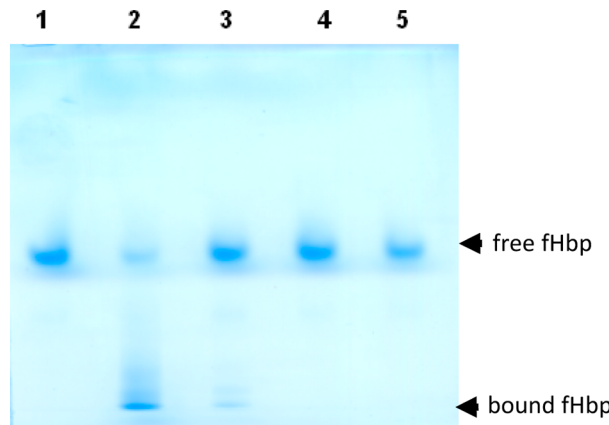


Figure 2. Native PAGE of 10 μg of fHbp alone (lane 1) and fHbp in the presence of different ferric siderophores at a 1:1 molar ratio: Fe^{III}(Ent)³⁻ (lane 2), Fe^{III}(Sal)³⁻ (lane 3), Fe^{III}(Yers) (lane 4), and Fe^{III}(Aer) (lane 5).

preincubation of fHbp with aerobactin and yersiniabactin did not alter its electrophoretic pattern. The faster migration of the fHbp–Fe^{III}(Ent)³⁻ complex was likely due to an altered electrostatic potential on the fHbp surface when it was bound to enterobactin. We concluded therefore that fHbp was able to bind catecholates in vitro and that such interaction was more pronounced in the case of enterobactin.

SPR Binding Studies. To confirm the indications derived from native PAGE, we analyzed the binding affinity of Fe(Ent)³⁺ for immobilized fHbp by surface plasmon resonance

(SPR). $\text{Fe}^{\text{III}}(\text{Yers})$ and $\text{Fe}^{\text{III}}(\text{Aer})$ were also included in the analysis as negative controls.

SPR profiles clearly demonstrated binding of fHbp to $\text{Fe}^{\text{III}}(\text{Ent})^{3-}$, while no interaction was observed with $\text{Fe}^{\text{III}}(\text{Yers})$ and $\text{Fe}^{\text{III}}(\text{Aer})$ (Figure 3A). The fHpb affinity was specific for the $\text{Fe}^{\text{III}}(\text{Ent})^{3-}$ form, as no interaction was observed with the apo-Ent form (Figure 3B). Of interest, the affinity for $\text{Fe}^{\text{III}}(\text{Ent})^{3-}$ appeared to be maintained by the gonococcal orthologue of fHbp, which did not show any binding to domains 6 and 7 of fH (Figure 3C).

Titrations with increasing concentrations of $\text{Fe}^{\text{III}}(\text{Ent})^{3-}$ (ranging from 2.2 to 240 μM) were performed on immobilized fHbp from the meningococcal MC58 strain (variant 1). The shape of the curves prevented fitting the sensorgrams with any Biacore T100 Evaluation kinetic models. However, steady-state analysis of the curves provided an estimated value for the thermodynamic dissociation constant (K_D) of 35 μM for binding of $\text{Fe}^{\text{III}}(\text{Ent})^{3-}$ to fHbp (Figure 4). Results for fHbp variants 2 and 3, tested using fHbp from strains 2996 and M1239, respectively, showed comparable affinities and similar profiles of association and dissociation behavior (Table S3 of the Supporting Information).

NMR Mapping of the fHbp–Enterobactin Interaction.

The interaction between $\text{Fe}^{\text{III}}(\text{Ent})^{3-}$ and fHbp was further characterized by NMR by analyzing the chemical shift perturbations in the $^1\text{H}-^{15}\text{N}$ HSQC spectrum of the protein caused by the addition of apo-Ent and $\text{Fe}^{\text{III}}(\text{Ent})^{3-}$. Analysis of the interaction with $\text{Fe}^{\text{III}}(\text{Yers})$ was also included as a negative control.

Addition of increasing amounts of paramagnetic $\text{Fe}^{\text{III}}(\text{Ent})^{3-}$ to ^{15}N -labeled fHbp resulted in a progressive increase in the line widths of Gly148, Arg149, Ala150, Thr151, Arg153, Lys230, Gln232, Lys254, and Gln255 NH cross-peaks in the $^1\text{H}-^{15}\text{N}$ HSQC spectra. Such signals disappeared at an fHbp: $\text{Fe}^{\text{III}}(\text{Ent})^{3-}$ molar ratio of 1:5 (Figure S1 of the Supporting Information). The Fe^{III} bound to enterobactin is highly paramagnetic, being in a high-spin $S = \frac{5}{2}$ state. This added a large contribution to the nuclear relaxation rates, thus increasing signal line widths beyond detection.

The binding to fHbp was very specific for $\text{Fe}^{\text{III}}(\text{Ent})^{3-}$ as no effects were detected on the NMR spectra when apo-Ent was added to the sample (Figure S2 of the Supporting Information). No perturbations were detected in the NMR spectra when a solution of FeCl_3 was added, indicating that Fe^{III} ions alone were not directly coordinated by the protein.

The same spectral changes observed upon addition of $\text{Fe}^{\text{III}}(\text{Ent})^{3-}$ were restored either when a solution of FeCl_3 was added to an fHbp/apo-Ent mixture or when apo-Ent was added to an fHbp/ Fe^{III} mixture (Figure S2 of the Supporting Information). Indeed, apo-Ent readily formed a complex with Fe^{III} , generating $\text{Fe}^{\text{III}}(\text{Ent})^{3-}$, which was the only form able to bind to fHbp.

The specificity of $\text{Fe}^{\text{III}}(\text{Ent})^{3-}$ for fHbp was confirmed by the absence of interactions of fHbp with other siderophores such as $\text{Fe}^{\text{III}}(\text{Yers})^{3-}$. In line with the absence of binding observed through SPR analysis, no changes were observed in the $^1\text{H}-^{15}\text{N}$ HSQC fHbp spectrum upon addition of $\text{Fe}^{\text{III}}(\text{Yers})$ (Figure S3 of the Supporting Information).

The protein residues involved in the protein–small molecule interaction were mapped onto the NMR structure (PDB entry 2KC0). All residues, whose NH cross-peak disappeared upon addition of $\text{Fe}^{\text{III}}(\text{Ent})^{3-}$, were located on the C-terminal domain (Figure 5). A multiple alignment of the different

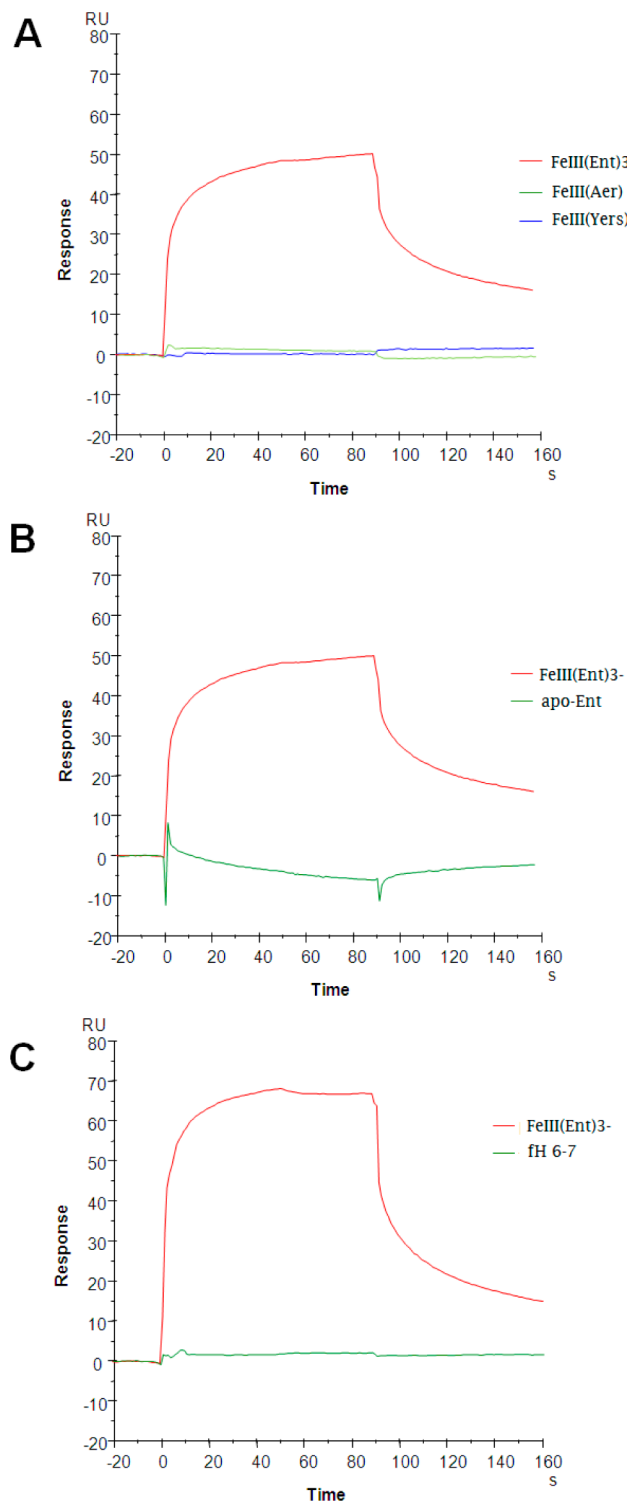


Figure 3. Solution-phase $\text{Fe}^{\text{III}}(\text{Ent})^{3-}$ –fHbp binding measured by surface plasmon resonance. (A) Representative sensorgrams show the response over time [resonance units (RU)] during the binding at neutral pH of $\text{Fe}^{\text{III}}(\text{Ent})^{3-}$ to immobilized recombinant fHbp from strain MC58. $\text{Fe}^{\text{III}}(\text{Yers})^{3-}$ and $\text{Fe}^{\text{III}}(\text{Aer})$ are not able to bind fHbp. (B) Binding to enterobactin is specific for $\text{Fe}^{\text{III}}(\text{Ent})^{3-}$ as no interaction is observed with the apo-Ent form. (C) Binding properties of the the *N. gonorrhoeae* fHbp allele. The protein is able to bind to $\text{Fe}^{\text{III}}(\text{Ent})^{3-}$ (red) but does not have affinity for domains 6 and 7 of human factor H (green), which contain the interaction site with the meningococcal allele.²⁰

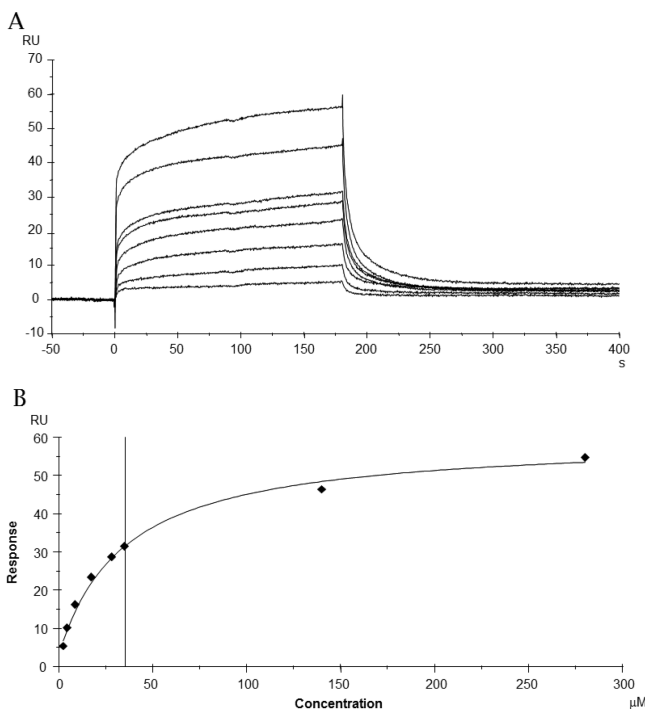


Figure 4. SPR analysis of the fHbp–siderophore interactions. (A) $\text{Fe}^{\text{III}}(\text{Ent})^{3-}$ was injected over immobilized fHbp from the MC58 strain. The SPR curves demonstrated a clear dose–response relationship. The titration included $\text{Fe}^{\text{III}}(\text{Ent})^{3-}$ concentrations from 2.2 to 280 μM . (B) Steady-state binding analysis of the sensorgrams from panel A allowed determination of the equilibrium binding constant (K_D) of 35 μM for the $\text{Fe}^{\text{III}}(\text{Ent})^{3-}$ –fHbp interaction. The vertical solid line indicates the concentration of the calculated K_D value.

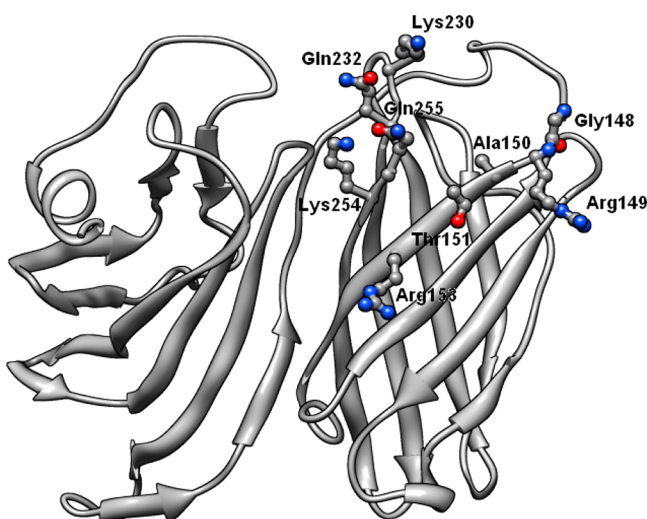


Figure 5. fHbp–enterobactin interaction site identified by NMR. Surface-accessible residues (Gly148, Arg149, Ala150, Thr151, Arg153, Lys230, Gln232, Lys254, and Gln255) whose amide signals were perturbed upon the addition of $\text{Fe}^{\text{III}}(\text{Ent})^{3-}$ (see the text for details) are represented as balls and sticks. This figure was prepared with UCSF Chimera (<http://www.cgl.ucsf.edu/chimera/>).

fHbp variants showed that such amino acids were generally well conserved or carried conservative substitutions, enforcing the hypothesis that they could form a functional site of the protein surface (Figure 6).

The 200 docking solutions of models of the fHbp– $\text{Fe}^{\text{III}}(\text{Ent})^{3-}$ adduct could be divided into two clusters. In each case, $\text{Fe}^{\text{III}}(\text{Ent})^{3-}$ interacted with the same region of the protein, and the location of enterobactin in the two clusters was comparable, with only minor differences in the conformations of the three catecholate rings (Figure S4 of the Supporting Information). From the analysis of the energetic and scoring functions, both clusters had similar energy term values, numbers of violations, and buried surface areas, although cluster 1 showed a slightly lower HADDOCK score (Table S2 of the Supporting Information). The average structure of this cluster is shown in Figure 7. fHbp binds $\text{Fe}^{\text{III}}(\text{Ent})^{3-}$ in a solvent-exposed area of its surface, arranging the side chain of two positively charged residues (Lys230 and Arg149) between two of the three catecholate rings of $\text{Fe}^{\text{III}}(\text{Ent})^{3-}$. Additional stabilizing hydrophobic contacts were made by residues lining the interaction site, such as Tyr152, Phe172, and Ala231 and $\text{Fe}^{\text{III}}(\text{Ent})^{3-}$. Hydrogen bonds between the carbonyl oxygen of the amide connecting the catecholate to the backbone of enterobactin molecule and both the side chain and the amide group of the Thr151 were found in all the docking solutions (Figure S5 of the Supporting Information).

DISCUSSION

Bacterial pathogens require iron for growth; however, in their host, the level of free iron is tightly regulated and is not readily available. For this reason, microbes have evolved a number of iron uptake systems to ensure access to the level of iron that is required for their survival. For example, *N. gonorrhoeae* and *N. meningitidis* can sequester iron from hemoglobin by means of major iron-regulated proteins.^{36,37} Other bacteria, including *E. coli*, *Salmonella*, *Yersinia*, *Bacillus*, *Vibrio*, and *Mycobacterium* spp., secrete siderophores, which are high-affinity compounds that chelate ferric iron from the environment. In other cases, bacteria can use siderophores produced by other microorganisms (xenosiderophores). *N. meningitidis* expresses a number of surface receptors for host iron-containing proteins, including transferrin and lactoferrin.^{37,38} Additionally, although its ability to produce siderophores has not been demonstrated, the meningococcus expresses the outer membrane siderophore receptor FrpB, whose orthologue in *N. gonorrhoeae*, named FetA, has been characterized as a TonB-dependent receptor capable of binding a range of catecholate siderophores, including enterobactin,³⁹ salmochelin, and dihydroxybenzoylserine.⁴⁰ This raised the question of whether the meningococcus can actually take up iron through xenosiderophores and motivated our search for possible novel siderophore receptors.

The structural similarity of the fHbp C-terminal domain to lipocalins suggested that fHbp could play the role of a siderophore receptor. As siderophores have extremely heterogeneous structures, we probed the hypothesis by examining the affinity of fHbp for four molecules identified as being representative of the main chemical classes. i.e., catecholates, hydroxamates, and mixed. In particular, we focused the choice on two catecholates (enterobactin and salmochelin), the hydroxamate aerobactin and the mixed-type yersiniabactin, all of them known to be produced by pathogenic bacteria.²⁷ We found that fHbp was able to bind *in vitro* $\text{Fe}^{\text{III}}(\text{Ent})^{3-}$, a xenosiderophore produced by *E. coli* and *Salmonella* spp.⁴¹ NMR mapping revealed that the site of binding interaction with enterobactin was clearly distinct from the zone of the fHbp surface that is known to interact with factor H. Docking calculations performed with HADDOCK suggest that the ferric

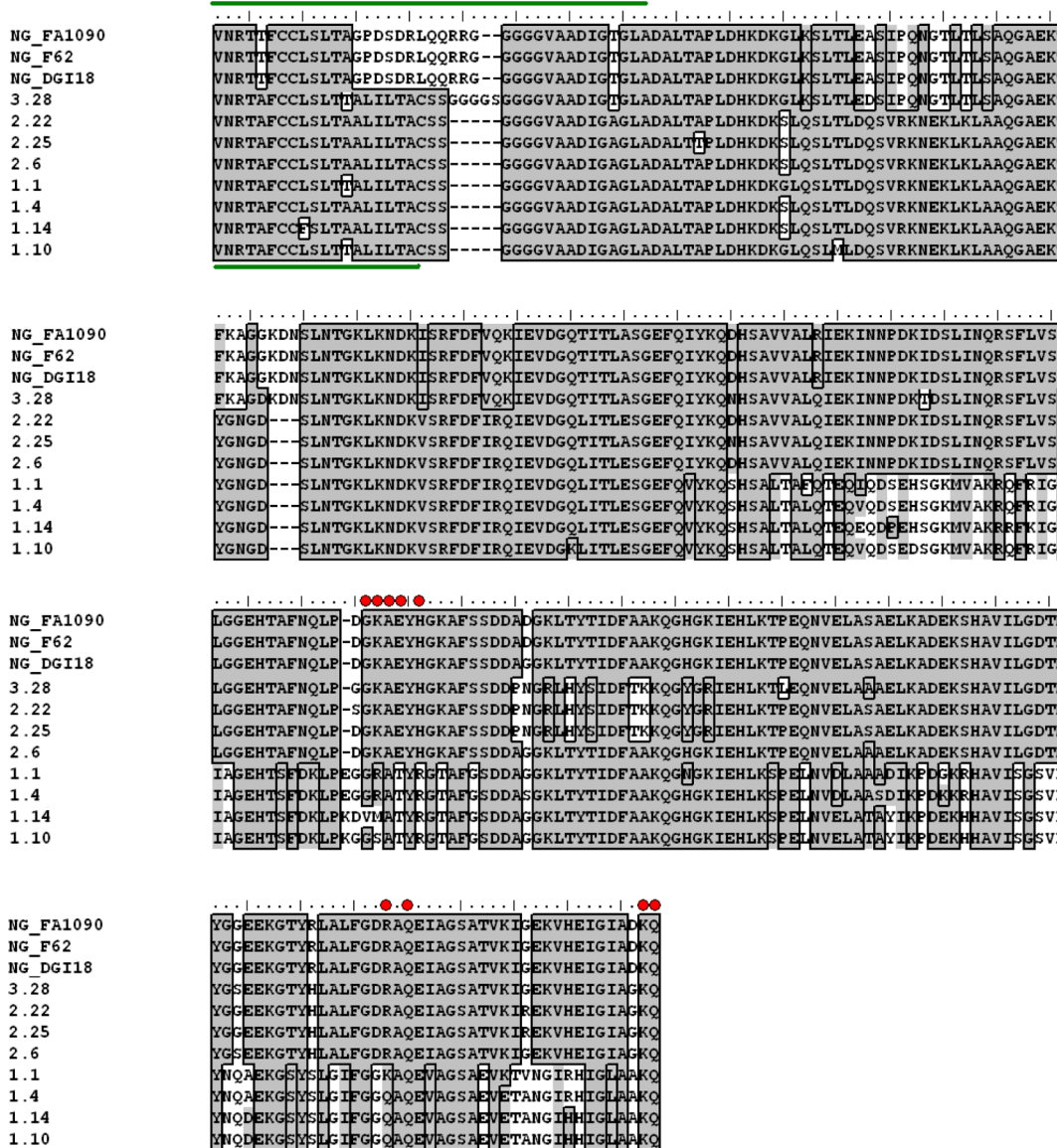


Figure 6. Multiple-sequence alignment of different fHbp variants. Meningococcal alleles previously identified as being representative of the natural variability (15) are labeled from 1.1 to 3.28 in accordance with the nomenclature adopted in the public fHbp database (<http://www.neisseria.org>). Gonococcal sequences were retrieved from the complete genome sequences of strains FA1090 (entry YP_207214), F62 (entry ZP_06641974), and DGI18 (entry ZP_04720259) filed in the protein section of the National Center for Biotechnology Information public database (<http://www.ncbi.nlm.nih.gov/protein>). Residues forming the enterobactin binding site are marked by red circles. Putative signal peptides are evidenced with green bars.

siderophore rests at the surface of one extremity of the C-terminal β barrel.

The HADDOCK model of the fHbp–Fe^{III}(Ent)³⁻ adduct showed several analogies to the already characterized complexes of enterobactin with NGAL and Q83 lipocalins.^{42,43} Both NGAL and Q83 display a highly conserved structural fold constituted by an eight-stranded antiparallel β barrel, which encloses a cup-shaped Fe^{III}(Ent)³⁻ binding site. However, Fe^{III}(Ent)³⁻ interacted less deeply in the β barrel of fHbp where the binding site is more shallow. As a consequence, in the fHbp–Fe^{III}(Ent)³⁻ adduct, one of the catecholate rings did not have any contact with the protein and was completely exposed to the solvent (Figure S5 of the Supporting Information). This represented a major difference versus what has been observed in NGAL– and Q83–Fe^{III}(Ent)³⁻ adducts, in which the three catecholate rings are deeply buried within the positively

charged pocket. The differences in binding could reflect the different affinity observed between the fHbp–Fe^{III}(Ent)³⁻ adduct and the other two lipocalin–enterobactin complexes, whose K_D values were both estimated to be in the nanomolar range.^{42,43}

All of the three fHbp variants analyzed bind Fe^{III}(Ent)³⁻ with similar affinities (Table S3 of the Supporting Information). The fHbp residues identified in the model as interacting with Fe^{III}(Ent)³⁻ via their side chains (Figure S5 of the Supporting Information) were well conserved among the fHbp variants or subjected to conservative substitutions (Figure 6). In particular, Gln232 and Gln255, both invariant in the sequence alignment, established polar interactions with enterobactin O11 and O13 atoms, respectively. The side chains of Arg230 and Arg149 were arranged between the catecholate rings of Fe^{III}(Ent)³⁻, indicating that positively charged amino acids within fHbp

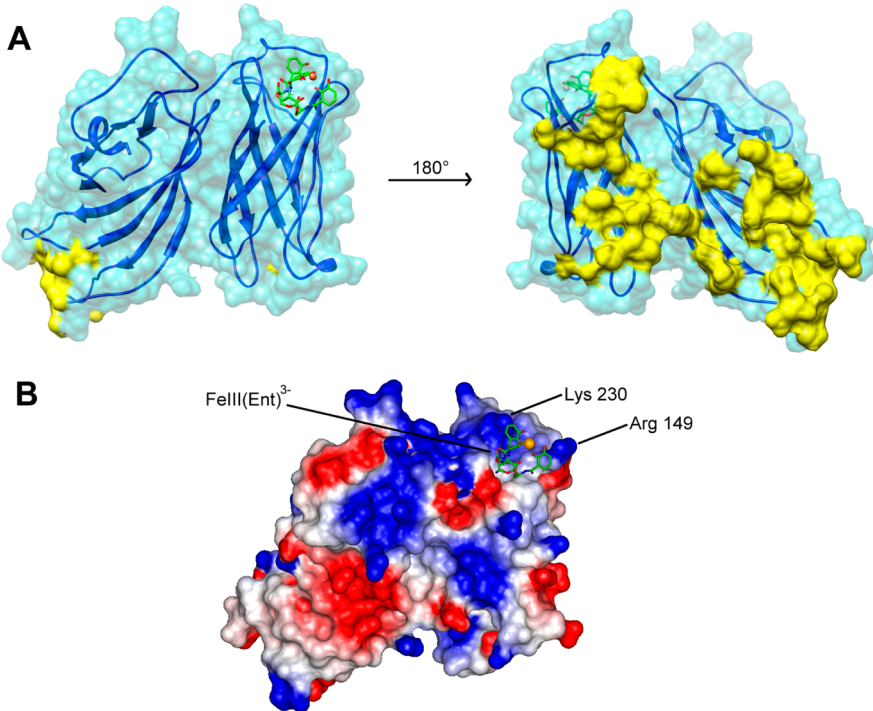


Figure 7. Lowest-score structural model of the fHbp–Fe^{III}(Ent)^{3–} complex. The Fe^{III}(Ent)^{3–} molecule is shown as sticks (green for carbon, blue for nitrogen, red for oxygen, and an orange sphere for the Fe atom). The surface of the protein is colored dark green. Residues involved in the interaction with human fH are mapped in yellow onto the protein surface. (A) Electrostatic potential surface of fHbp. (B) The Fe^{III}(Ent)^{3–} molecule is also shown. Key residues involved in electrostatic and cation–π interactions with Fe^{III}(Ent)^{3–} are labeled on the protein electrostatic surface.

recognize the catechol groups of Fe^{III}(Ent)^{3–} by interacting with their aromatic electron density and forming cation–π bonds. Moreover, in a manner different from that of neutral apo-Ent, the formation of the tris-catecholate coordination structure in Fe^{III}(Ent)^{3–} can maximize cationic–π and Coulombic interactions within the fHbp binding site. The majority of fHbp subvariants have positively charged residues (arginine or lysine) at position 230 and 149 (Figure 6). However, the observation that in a few cases (fHbp alleles 1.14 and 1.10) nonconservative substitutions can occur suggests that the network of interactions stabilizing the enterobactin could be different in some alleles or, as an alternative, that such alleles might have a different affinity for enterobactin.

Additional stabilizing hydrophobic contacts were made by residues lining the interaction site, such as Tyr152 and Phe172, both of which are strictly conserved within the three variants (Figure 6). The line widths of the amide signal of Tyr152 in particular increased upon addition of paramagnetic Fe^{III}(Ent)^{3–}. Overall, the model suggests that both the charge and the structure of Fe^{III}(Ent)^{3–} are responsible for fHbp recognition, and this could explain why Fe^{III}(Yers) and Fe^{III}(Aer), both lacking catecholate rings, do not bind fHbp because of the neutral nature of their ferric complexes and the lack of aromatic binding units.

The use of *E. coli* siderophores in *N. gonorrhiae* has been well documented.⁴⁰ It was not therefore unforeseen that the gonococcal fHbp homologue was also able to bind enterobactin. The ability of meningococcal fHbp to bind enterobactin was instead somewhat surprising, considering that the niches colonized by the meningococcus render it improbable that it has evolved to exploit siderophores *in vivo* that are produced by Enterobacteria.

It has already been pointed out that the gonococcal fHbp differs at the N-terminus compared to meningococcal variants, and it has been speculated that the gonococcal polypeptide, which lacks a signal peptidase II motif, remains confined in the cytoplasm.⁴⁴ However, sequence inspection suggests that gonococcal fHbp can be recognized by a twin-arginine translocation system,⁴⁵ which could direct it to the periplasmic space (Figure 6). This observation leads to the intriguing hypothesis that the same protein differentiated its activity and function in *N. meningitidis* and *N. gonorrhiae*, by modulating its subcellular localization and affinity for different substrates. In the gonococcus, the protein could be located in the periplasm where it could exert a role in iron uptake, whereas the surface-located orthologue in *N. meningitidis* mediates fH binding to allow escape of the host immune system. On the other hand, SPR indicated that the recombinant gonococcal fHbp allele is unable to bind to fH. This raises the question of whether fHbp is an appropriate name for the gonococcal orthologue and suggests that molecule transport could represent its predominant role.

Such considerations cannot, however, lead us to exclude the possibility that the maintenance of the ability to bind siderophores represents an advantage also for the meningococcus. The presence in the meningococcal genome of a gene encoding FrpB, the orthologue of the gonococcal enterobactin receptor FtaA, seems to suggest that the maintenance of potential receptors for iron scavenging could provide a useful reservoir that allows the bacterium to rapidly adapt to possible environmental changes.

The biological significance of binding of fHbp to Fe^{III}(Ent)^{3–} in meningococcus remains to be investigated. The low affinity of this complex suggests that fHbp could represent the primitive function of fHbp on which fH binding successively

prevailed to enhance the fitness of the bacterium in human blood.

As an alternative, fHbp could physiologically bind a different currently unknown siderophore or a modification product of ferric enterobactin. It has been recently demonstrated that in response to colonization by both Gram-positive and Gram-negative pathogens the mammalian nasal mucosa reacts by secreting lipocalin_2 (Lpn2), a potent iron scavenger of apo and ferric enterobactin.^{46,47} Lpn2 acts as a bacteriostatic agent, silencing one of the most effective ways to acquire iron within the host and providing a natural barrier that bacteria have to overcome to successfully colonize the nasal mucosa. We could therefore speculate that, perhaps to evade the effects of Lpn2, *N. meningitidis* evolved mechanisms to escape the strict dependence on enterobactin for iron acquisition, by using of alternative and/or modified siderophores or improving the removal of iron from various human proteins such as lactoferrin, transferrin, and hemoglobin.³⁸

In conclusion, we reported here for the first time evidence that fHbp of *N. meningitidis* and its counterpart in *N. gonorrhoeae* can bind enterobactin *in vitro*. The ultimate goal of this study is to explore new aspects of the fHbp functionality and contribute to the identification of new targets for drug design.

■ ASSOCIATED CONTENT

Supporting Information

¹H-¹⁵N HSQC spectrum of 0.5 mM fHbp in the absence and presence of 1.5 equiv of Fe^{III}(Ent)³⁻ (Figure S1), ¹H-¹⁵N HSQC spectrum of 0.5 mM fHbp superimposed with fHbp in the presence of 1.5 equiv of apo-Ent and with an fHbp/apo-Ent mixture in the presence of 1.5 equiv of FeCl₃ (Figure S2), ¹H-¹⁵N HSQC spectrum of 0.5 mM fHbp superimposed with fHbp in the presence of 1.5 equiv of Fe^{III}(Yers) (Figure S3), overlay of the Fe^{III}(Ent)³⁻ models generated with HADDOCK (Figure S4), contacts between fHbp and Fe^{III}(Ent)³⁻ (Figure S5), a list of the active and passive residues of fHBP used to generate the ambiguous interaction restraints for the docking calculation (Table S1), and statistics about the cluster of the structural model of the fHbp-Fe^{III}(Ent)³⁻ complex, obtained via docking calculations (Table S2). This material is available free of charge via the Internet at <http://pubs.acs.org>.

■ AUTHOR INFORMATION

Corresponding Author

*R.R.: Novartis Vaccines and Diagnostics S.r.l., Via Fiorentina 1, 53100 Siena, Italy; telephone, +39 0577 243414; fax, +39 0577 243564; e-mail, rino.rappuoli@novartis.com. L.B.: Magnetic Resonance Center, University of Florence, Via L. Sacconi 6, 50019 Sesto Fiorentino, Italy; telephone, +39 055 4574263; fax, +39 055 4574253; e-mail, banci@cerm.unifi.it.

Author Contributions

D.V. and M.A.G. contributed equally to this work.

Funding

This work was supported by the BIOVAX grant funded by Piano Operativo Regionale (POR) of Regione Toscana.

Notes

The authors declare no competing financial interest.

■ ACKNOWLEDGMENTS

We thank Dr. Susan Lea and Christoph Tang (Centre for Molecular Microbiology and Infection, Imperial College,

London, U.K.), who kindly provided recombinant purified domains 6 and 7 of human factor H.

Thanks are due also to Mr. Giorgio Corsi for the graphics.

■ ABBREVIATIONS

fH, factor H; fHbp, factor H binding protein; NMR, nuclear magnetic resonance; SPR, surface plasmon resonance; IPTG, isopropyl thio-β-D-galactopyranoside; Fe^{III}(Ent)³⁻, ferric enterobactin; apo-Ent, iron free enterobactin; Fe^{III}(Yers)³⁻, ferric yersiniabactin; Fe^{III}(Aer)³⁻, ferric aerobactin; PDB, Protein Data Bank.

■ REFERENCES

- Harrison, L. H., Trotter, C. L., and Ramsay, M. E. (2009) Global epidemiology of meningococcal disease. *Vaccine* 27 (Suppl. 2), B51-B63.
- Schuchat, A., Robinson, K., Wenger, J. D., Harrison, L. H., Farley, M., Reingold, A. L., Lefkowitz, L., and Perkins, B. A. (1997) Bacterial Meningitis in the United States in 1995. *N. Engl. J. Med.* 337, 970-976.
- Rosenstein, N. E., Perkins, B. A., Stephens, D. S., Popovic, T., and Hughes, J. M. (2001) Meningococcal Disease. *N. Engl. J. Med.* 344, 1378-1388.
- Finne, J., Bitter-Suermann, D., Goridis, C., and Finne, U. (1987) An IgG monoclonal antibody to group B meningococci cross-reacts with developmentally regulated polysialic acid units of glycoproteins in neural and extraneuronal tissues. *J. Immunol.* 138, 4402-4407.
- Nedelec, J., Boucraut, J., Garnier, J. M., Bernard, D., and Rougon, G. (1990) Evidence for autoimmune antibodies directed against embryonic neural cell adhesion molecules (N-CAM) in patients with group B meningitis. *J. Neuroimmunol.* 29, 49-56.
- Wyle, F. A., Artenstein, M. S., Brandt, B. L., Tramont, E. C., Kasper, D. L., Altieri, P. L., Berman, S. L., and Lowenthal, J. P. (1972) Immunologic Response of Man to Group B Meningococcal Polysaccharide Vaccines. *J. Infect. Dis.* 126, 514-522.
- Sadarangani, M., and Pollard, A. J. (2010) Serogroup B meningococcal vaccines an unfinished story. *Lancet Infect. Dis.* 10, 112-124.
- Pizza, M., Scarlato, V., Masignani, V., Giuliani, M. M., Aricò, B., Comanducci, M., Jennings, G. T., Baldi, L., Bartolini, E., Capecchi, B., Galeotti, C. L., Luzzi, E., Manetti, R., Marchetti, E., Mora, M., Nuti, S., Ratti, G., Santini, L., Savino, S., Scarselli, M., Storni, E., Zuo, P., Broeker, M., Hundt, E., Knapp, B., Blair, E., Mason, T., Tettelin, H., Wood, D. W., Jeffries, A. C., Saunders, N. J., Granoff, D. M., Venter, J. C., Moxon, E. R., Grandi, G., and Rappuoli, R. (2000) Identification of vaccine candidates against serogroup B meningococcus by whole-genome sequencing. *Science* 287, 1816-1820.
- Bai, X., Findlow, J., and Borrow, R. (2011) Recombinant protein meningococcal serogroup B vaccine combined with outer membrane vesicles. *Expert Opin. Biol. Ther.* 11, 969-985.
- Fletcher, L. D., Bernfield, L., Farley, J. E., Howell, A., Knauf, M., Ooi, P., Smith, R. P., Weise, P., Wetherell, M., Xie, X., Zagursky, R., Zhang, Y., and Zlotnick, G. W. (2004) Vaccine potential of the *Neisseria meningitidis* 2086 lipoprotein. *Infect. Immun.* 72, 2088-2100.
- Giuliani, M. M., Adu-Bobie, J., Comanducci, M., Aricò, B., Savino, S., Santini, L., Brunelli, B., Bambini, S., Biolchi, A., Capecchi, B., Cartoccia, E., Ciucchi, L., Di Marcello, F., Ferlicca, F., Galli, B., Luzzi, E., Masignani, V., Serruto, D., Veggi, D., Contorni, M., Morandi, M., Bartalesi, A., Cinotti, V., Mannucci, D., Titta, F., Ovidi, E., Welsch, J. A., Granoff, D., Rappuoli, R., and Pizza, M. (2006) A universal vaccine for serogroup B meningococcus. *Proc. Natl. Acad. Sci. U.S.A.* 103, 10834-10839.
- Jiang, H. Q., Hoiseth, S. K., Harris, S. L., McNeil, L. K., Zhu, D., Tan, C., Scott, A. A., Alexander, K., Mason, K., Miller, L., Dilva, I., Mack, M., Zhao, X. J., Pride, M. W., Andrew, L., Murphy, E., Hagen, M., French, R., Arora, A., Jones, T. R., Jansen, K. U., Zlotnick, G. W., and Anderson, A. S. (2010) Broad vaccine coverage predicted for a bivalent recombinant factor H binding protein based vaccine to

- prevent serogroup B meningococcal disease. *Vaccine* 28 (37), 6086–6093.
- (13) Scarselli, M., Aricò, B., Brunelli, B., Savino, S., Di Marcello, F., Palumbo, E., Veggi, D., Ciucchi, L., Cartocci, E., Bottomley, M. J., Malito, E., Lo Surdo, P., Comanducci, M., Giuliani, M. M., Cantini, F., Dragonetti, S., Colaprico, A., Doro, F., Giannetti, P., Pallaoro, M., Brogioni, B., Tontini, M., Hilleringmann, M., Nardi-Dei, V., Banci, L., Pizza, M., and Rappuoli, R. (2011) Rational Design of a Meningococcal Antigen Inducing Broad Protective Immunity. *Sci. Transl. Med.* 3, 91ra62.
- (14) Massignani, V., Comanducci, M., Giuliani, M. M., Bambini, S., Adu-Bobie, J., Aricò, B., Brunelli, B., Pieri, A., Santini, L., Savino, S., Serruto, D., Litt, D., Kroll, S., Welsch, J. A., Granoff, D. M., Rappuoli, R., and Pizza, M. (2003) Vaccination against *Neisseria meningitidis* Using Three Variants of the Lipoprotein GNA1870. *J. Exp. Med.* 197, 789–799.
- (15) Seib, K. L., Brunelli, B., Brogioni, B., Palumbo, E., Bambini, S., Muzzi, A., DiMarcello, F., Marchi, S., van der Ende, A., Aricò, B., Savino, S., Scarselli, M., Comanducci, M., Rappuoli, R., Giuliani, M. M., and Pizza, M. (2011) Characterization of diverse subvariants of the meningococcal factor H (fH) binding protein for their ability to bind fH, to mediate serum resistance, and to induce bactericidal antibodies. *Infect. Immun.* 79, 970–981.
- (16) Józsi, M., and Zipfel, P. F. (2008) Factor H family proteins and human diseases. *Trends Immunol.* 29, 380–387.
- (17) Hakobyan, S., Tortajada, A., Harris, C. L., de Córdoba, S. R., and Morgan, B. P. (2010) Variant-specific quantification of factor H in plasma identifies null alleles associated with atypical hemolytic uremic syndrome. *Kidney Int.* 78, 782–788.
- (18) Rodríguez de Córdoba, S., Esparza-Gordillo, J., Goicoechea de Jorge, E., Lopez-Trascasa, M., and Sánchez-Corral, P. (2004) The human complement factor H: Functional roles, genetic variations and disease associations. *Mol. Immunol.* 41, 355–367.
- (19) Schneider, M. C., Prosser, B. E., Caesar, J. J. E., Kugelberg, E., Li, S., Zhang, Q., Quoraishi, S., Lovett, J. E., Deane, J. E., Sim, R. B., Roversi, P., Johnson, S., Tang, C. M., and Lea, S. M. (2009) *Neisseria meningitidis* recruits factor H using protein mimicry of host carbohydrates. *Nature* 458, 890–893.
- (20) Madico, G., Welsch, J. A., Lewis, L. A., McNaughton, A., Perlman, D. H., Costello, C. E., Ngampasutadol, J., Vogel, U., Granoff, D. M., and Ram, S. (2006) *J. Immunol.* 177, 501–510.
- (21) Cendron, L., Veggi, D., Girardi, E., and Zanotti, G. (2011) Structure of the uncomplexed *Neisseria meningitidis* factor H-binding protein fHbp (rLP2086). *Acta Crystallogr.* 67, S31–S35.
- (22) Mascioni, A., Bentley, B. E., Camarda, R., Dilts, D. A., Fink, P., Gusarova, V., Hoiseth, S. K., Jacob, J., Lin, S. L., Malakian, K., McNeil, L. K., Mininni, T., Moy, F., Murphy, E., Novikova, E., Sigethy, S., Wen, Y., Zlotnick, G. W., and Tsao, D. H. (2009) Structural Basis for the Immunogenic Properties of the Meningococcal Vaccine Candidate LP2086. *J. Biol. Chem.* 284, 8738–8746.
- (23) Cantini, F., Veggi, D., Dragonetti, S., Savino, S., Scarselli, M., Romagnoli, G., Pizza, M., Banci, L., and Rappuoli, R. (2009) Solution Structure of the Factor H-binding Protein, a Survival Factor and Protective Antigen of *Neisseria meningitidis*. *J. Biol. Chem.* 284, 9022–9026.
- (24) Esposito, V., Musi, V., de Chiara, C., Veggi, D., Serruto, D., Scarselli, M., Kelly, G., Pizza, M., and Pastore, A. (2011) Structure of the C-terminal Domain of *Neisseria* Heparin Binding Antigen (NHBA), One of the Main Antigens of a Novel Vaccine against *Neisseria meningitidis*. *J. Biol. Chem.* 286, 41767–41775.
- (25) Russell, E. B. (2000) The bacterial lipocalins. *Biochim. Biophys. Acta* 1482, 73–83.
- (26) Grzyb, J., Latowski, D., and Strzalka, K. (2006) Lipocalins: A family portrait. *J. Plant Physiol.* 163, 895–915.
- (27) Schalk, I. J., Hannauer, M., and Braud, A. (2011) New roles for bacterial siderophores in metal transport and tolerance. *Environ. Microbiol.* 13, 2844–2854.
- (28) de Vries, S. J., van Dijk, A. D., Krzeminski, M., van Dijk, M., Thureau, A., Hsu, V., Wassenaar, T., and Bonvin, A. M. (2007) HADDOCK versus HADDOCK: New features and performance of HADDOCK2.0 on the CAPRI targets. *Proteins* 69, 726–733.
- (29) Schüttelkopf, A. W., and van Aalten, D. M. (2004) PRODRG: A tool for high-throughput crystallography of protein-ligand complexes. *Acta Crystallogr. D60* (Part 8), 1355–1363.
- (30) Dominguez, C., Boelens, R., and Bonvin, A. (2003) HADDOCK: A protein-protein docking approach based on biochemical and/or biophysical information. *J. Am. Chem. Soc.* 125, 1731–1737.
- (31) Hubbard, S. J., and Thornton, J. M. (1993) NACCESS, Department of Biochemistry and Molecular Biology, University College London. London.
- (32) Arnesano, F., Banci, L., Bertini, I., and Bonvin, A. M. (2004) A docking approach to the study of copper trafficking proteins; interaction between metallochaperones and soluble domains of copper ATPases. *Structure* 12, 669–676.
- (33) D'Onofrio, M., Gianolio, E., Cecconi, A., Arena, F., Zanzoni, S., Fushman, D., Aime, S., Molinari, H., and Assfalg, M. (2012) High relaxivity supramolecular adducts between human-liver-fatty-acid-binding protein and amphiphilic Gd(III) complexes: Structural basis for the design of intracellular targeting MRI probes. *Chemistry* 18, 9919–9928.
- (34) Tomaselli, S., Ragona, L., Zetta, L., Assfalg, M., Ferranti, P., Longhi, R., Bonvin, A. M., and Molinari, H. (2007) NMR-based modeling and binding studies of a ternary complex between chicken liver bile acid binding protein and bile acids. *Proteins* 69, 177–191.
- (35) van Dijk, A. D. J., Ciofi-Baffoni, S., Banci, L., Bertini, I., Boelens, R., and Bonvin, A. M. (2007) Modeling protein complexes involved in the cytochrome c oxidase copper delivery pathway. *J. Proteome Res.* 6, 1530–1539.
- (36) Banerjee, S., Siburt, C. J., Mistry, S., Noto, J. M., De Armond, P., Fitzgerald, M. C., Lambert, L. A., Cornelissen, C. N., and Crumbliss, A. L. (2012) Evidence of Fe³⁺ interaction with the plug domain of the outer membrane transferrin receptor protein of *Neisseria gonorrhoeae*: Implications for Fe transport. *Metallomics*, 361–372.
- (37) Calmettes, C., Alcantara, J., Yu, R. H., Schryvers, A. B., and Moraes, T. F. (2012) The structural basis of transferrin sequestration by transferrin-binding protein B. *Nat. Struct. Mol. Biol.* 19, 358–360.
- (38) Perkins-Balding, D., Ratliff-Griffin, M., and Stojiljkovic, I. (2004) Iron Transport Systems in *Neisseria meningitidis*. *Microbiol. Mol. Biol. Rev.* 68, 154–171.
- (39) Carson, S. D. B., Klebba, P. E., Newton, S. M. C., and Sparling, P. F. (1999) Ferric Enterobactin Binding and Utilization by *Neisseria gonorrhoeae*. *J. Bacteriol.* 181, 2895–2901.
- (40) Hollander, A., Mercante, A. D., Shafer, W. M., and Cornelissen, C. N. (2011) The Iron-Repressed, AraC-Like Regulator MpeR Activates Expression of fetA in *Neisseria gonorrhoeae*. *Infect. Immun.* 79, 4764–4776.
- (41) Raymond, K. N., Dertz, E. A., and Kim, S. S. (2003) Enterobactin: An archetype for microbial iron transport. *Proc. Natl. Acad. Sci. U.S.A.* 100, 3584–3588.
- (42) Abergel, R. J., Clifton, M. C., Pizarro, J. C., Warner, J. A., Shuh, D. K., Strong, R. K., and Raymond, K. N. (2008) The Siderocalin/Enterobactin Interaction: A Link between Mammalian Immunity and Bacterial Iron Transport. *J. Am. Chem. Soc.* 130, 11524–11534.
- (43) Coudeville, N., Hoetzinger, M., Geist, L., Kontaxis, G., Hartl, M., Bister, K., and Konrat, R. (2011) Lipocalin Q83 Reveals a Dual Ligand Binding Mode with Potential Implications for the Functions of Siderocalins. *Biochemistry* 50, 9192–9199.
- (44) Welsch, J., and Ram, S. (2008) Factor H and Neisseria pathogenesis. *Vaccine* 26, 140–145.
- (45) Berks, B., Sargent, F., and Palmer, T. (2000) The Tat protein export pathway. *Mol. Microbiol.* 35, 260–274.
- (46) Bachman, M. A., Miller, V. L., and Weiser, J. N. (2009) Mucosal lipocalin 2 has pro-inflammatory and iron-sequestering effects in response to bacterial enterobactin. *PLoS Pathog.* 5, e1000622.
- (47) Nelson, A. L., Barasch, J. M., Bunte, R. M., and Weiser, J. N. (2005) Bacterial colonization of nasal mucosa induces expression of

siderocalin, an iron-sequestering component of innate immunity. *Cell Microbiol.* 17, 1404–1417.